

PHYSICAL REVIEW B

CONDENSED MATTER AND MATERIALS PHYSICS

THIRD SERIES, VOLUME 57, NUMBER 7

15 FEBRUARY 1998-I

BRIEF REPORTS

Brief Reports are accounts of completed research which, while meeting the usual Physical Review B standards of scientific quality, do not warrant regular articles. A Brief Report may be no longer than four printed pages and must be accompanied by an abstract. The same publication schedule as for regular articles is followed, and page proofs are sent to authors.

Photonic band gaps in colloidal systems

R. Biswas, M. M. Sigalas, G. Subramania, and K.-M. Ho

Department of Physics and Astronomy, Ames Laboratory—U.S. DOE and Microelectronics Research Center, Iowa State University, Ames, Iowa 50011

(Received 18 July 1997)

Classes of colloidal dielectric systems are found with full three-dimensional photonic band gaps, using photonic band-structure calculations. The fcc structure composed from either high dielectric spheres or low dielectric spheres has three-dimensional band gaps and lower-frequency pseudogaps. The AB_2 structure has a higher-frequency pseudogap. [S0163-1829(98)00307-5]

A major thrust in the emerging field of photonic band gap (PBG) materials¹⁻³ has been to design and fabricate structures with three-dimensional photonic band gaps, at optical and near-infrared frequencies. Much interest has focused on colloidal systems, since these self-assemble into three-dimensional crystals with excellent long-range periodicity, at optical length scales. Photonic crystals with full PBG's can suppress spontaneous emission and control the lifetimes of chemical species in catalytic processes.³⁻⁵ The absorptionless colloid properties at optical wavelengths make them ideal for the first optical PBG crystals—which could lead to interesting optoelectronic applications.

Colloidal crystal growth produces inherently three-dimensional (3D) structures, a significant advantage over lithographic techniques which primarily produce two-dimensional patterns. Monodisperse colloidal suspensions of microspheres can self-order into crystalline structures at optical length scales.⁶⁻⁸ Colloidal epitaxy on a patterned substrate has produced macroscopic face-centered-cubic (fcc) colloidal crystals grown along the 100 direction.⁹ At low microsphere volume fractions ($\leq 5\%$), colloidal suspensions crystallize in the fcc (Ref. 7) and bcc (Ref. 8) lattices, that show optical stop bands along certain crystal directions. Binary colloidal mixtures of small and large microspheres show an entropically driven phase separation into a close-packed arrangement of larger spheres.^{10,11} Binary mixtures of hard spheres with a radius ratio of ~ 0.58 exhibit transitions to the complex AB_2 and AB_{13} crystal structures¹² with a high packing density (≥ 0.74) of the spheres. In spite of this wide diversity of colloidal crystals, the photonic proper-

ties of such systems are not well established. In this paper we predict crystal structures that have full 3D PBG's, and may be assembled from colloidal crystals.

Spontaneous emission depends both on density of the final photon states and the transition matrix element. Crystals with directional stop bands will generally not alter spontaneous emission unless the stop bands overlap in all directions of k space and lead to a pronounced change in the photon densities of states (DOS's). Two-dimensional photonic crystals are generally unsuitable for suppressing spontaneous emission, although they can be used to efficiently extract the emitted radiation.¹³ Hence we focus on three-dimensional PBG crystals here. Our calculations are based on the well-established method of vector-wave solutions of Maxwell's equations in a periodic dielectric structure utilizing plane-wave expansions of the E and H fields.^{2,14-16} This technique has been pivotal in predicting and designing three-dimensional PBG crystals with excellent agreement between theory and measurement.¹⁸ Densities of states are computed with the tetrahedron integration method using grids in the irreducible Brillouin zone.

We consider fcc structures composed of spheres (or more complex elements) of refractive index n_s , embedded in a background dielectric medium of refractive index n_b . f is the filling fraction of the dielectric n_s , and A the fcc lattice constant. Previous studies of the fcc structure of high dielectric spheres ($n_s > 1, n_b = 1$) found a pseudogap between the lowest bands.¹⁵ The finding in this paper is that the fcc structure can be modified to obtain a rich variety of *full* PBG's.

The fcc lattice of close-packed touching dielectric spheres

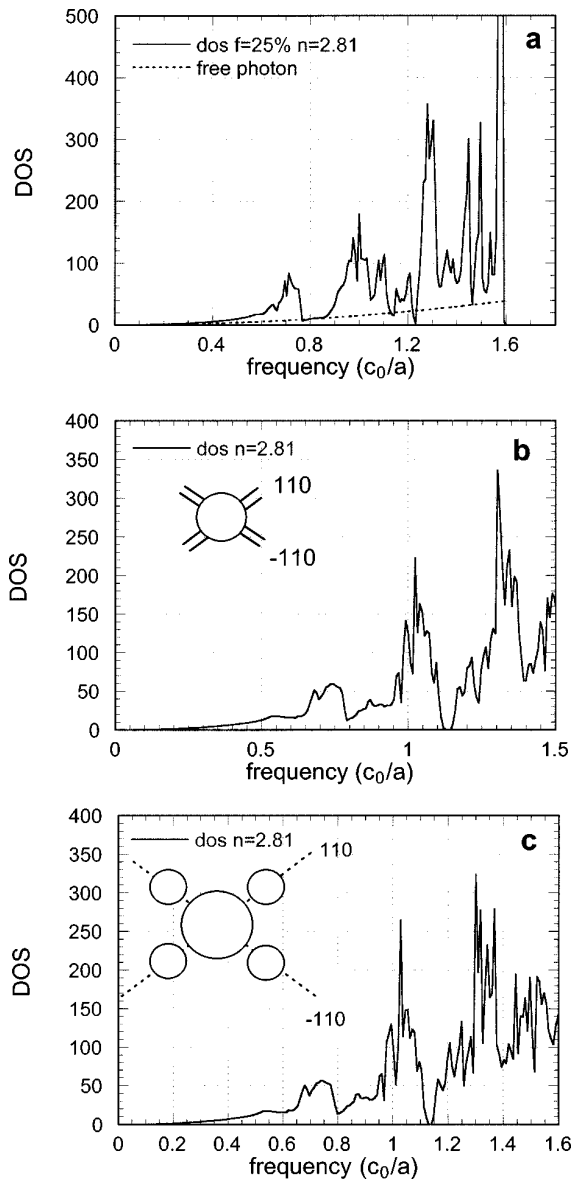


FIG. 1. (a) Photonic DOS for fcc lattice of high dielectric spheres in a low dielectric background, with a 25% dielectric filling ratio. For comparison, the free-photon DOS is shown by the dotted line. Frequencies are expressed in dimensionless units of c_0/A , where c_0 is the speed of light and A the fcc lattice constant. DOS is in units of photon states per unit cell. (b) Calculated photon DOS for the fcc lattice of dielectric spheres (radius R_b) connected by thin cylindrical rods (radius R_b) to form an interconnected network, displaying higher frequency gap. The filling ratio is 25%. (c) The photon DOS for fcc lattice of large dielectric spheres surrounded by smaller dielectric spheres (R_b) in the 110 directions. Each large sphere has 12 smaller spheres as neighbors for a filling ratio of 27%. As in (b), a higher-frequency gap is found.

has a featureless DOS (not shown),¹⁵ since the dielectric fraction is too large. If the fraction of dielectric is reduced to 25%, a photonic DOS [Fig. 1(a)] displays deep minima or pseudogaps at 0.8 and 1.22 (c_0/A). An index contrast of $n_s/n_b=2.81$ is used, appropriate for titania at optical wavelengths. The lower frequency pseudogap spans a wide frequency range ($\approx 15\%$), whereas the higher pseudogap is very narrow. At the higher “gap” the DOS is actually below

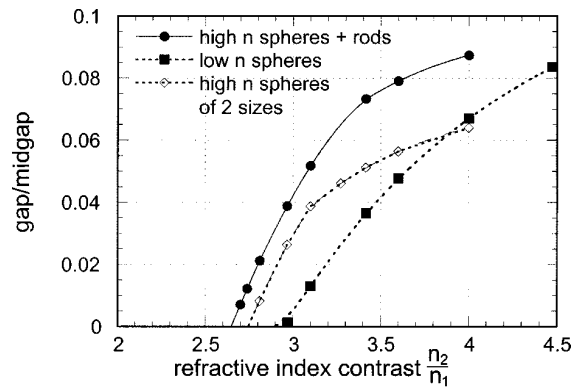


FIG. 2. The magnitude of the full 3D PBG as measured by the gap/midgap ratio as a function of the refractive index contrast. Results are for the high dielectric spheres connected by cylinders [Fig. 1(b)], the binary system of dielectric spheres [Fig. 1(c)], and low dielectric spheres in a high dielectric background (Fig. 3).

the free-photon DOS (dashed line, Fig. 1). The higher-frequency DOS was not considered in the earlier work. The close spacing between flatter higher bands¹⁷ generates rapid changes in the high-frequency DOS. Comparison with Mie scattering theory is applicable in the limit of small spheres. The low-frequency pseudogap at $0.8c_0/A$ is a remnant of the Mie resonances of a single sphere,¹⁵ where waves are strongly scattered.

Experimental synthesis of this structure may be feasible with coated spheres, having a high dielectric core (index n_s , and radius $R_i=0.7R$, where R is the sphere radius) enclosed by a suitable low dielectric outer coating (index n_b). Such spheres can then be close packed in the fcc structure.

This simple fcc structure can be modified to obtain a *full* PBG. If the spheres at the fcc lattice sites are connected by thin dielectric cylinders, generating a connected dielectric network with $f\approx 25\%$, we obtain a full higher frequency photonic gap [Fig. 1(b)]. The higher pseudogap found with spheres [Fig. 1(a)] opens into a full three-dimensional gap when the spheres are connected. This filling ratio is typical of the best 3D-PBG structures found previously. The extra rods provide connectivity of the dielectric structure, which is known to help the 3D gaps. The gap is robust for f ranging between 20–30%. The optimized gap occurs for a cylinder radius $R_{cyl}/A=0.048$ connecting spheres of radius $R_s/A=0.23$. The band gap remains open for contrasts of $n=2.81$ appropriate for titania. The minimum contrast needed to open the gap is 2.7, and the gap widens with increasing contrast (Fig. 2). This structure may be realized by enclosing large spheres by 12 smaller spheres and thermal treatment to fuse the smaller spheres into thin cylindrical rodlike connectors. This ball-and-stick structure may also be suitable for fabrication with the rapid laser prototyping.¹⁹ Connected 0.45μ -diameter titania spheres ($n=2.81$) gives a pseudogap of around 792 nm and a higher gap at 560 nm for the connected structure, and pseudogaps at 776 and 558 nm for the disconnected structure of spheres [Fig. 1(a)].

Another related fcc structure is composed of larger spheres ($R_a/A=0.23$) surrounded by 12 small spheres ($R_b/A=0.082$), that reside symmetrically between the larger spheres, in the 110 directions. The spheres do not touch, and the optimized f is 27% in this geometry. This structure has a

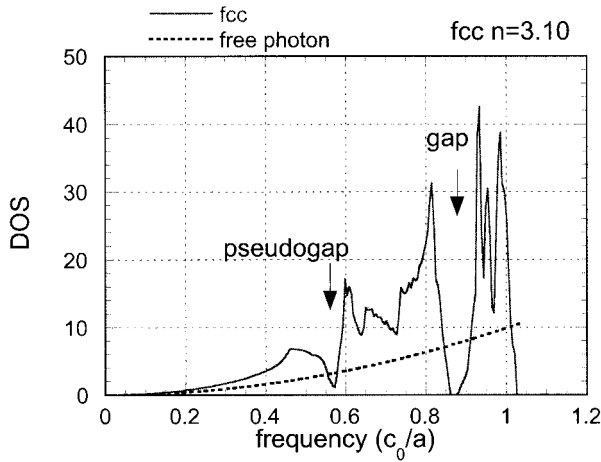


FIG. 3. The photonic densities of states for a close-packed fcc lattice of low dielectric spheres (refractive index n_1) in a high dielectric background (n_2). The calculated DOS is for a contrast $n_2/n_1=3.1$. The free-photon DOS (dashed line) is shown for comparison.

full gap [Fig. 1(c)], that is slightly reduced in magnitude from the case with spheres and rods. Fabrication of this structure is a candidate for binary colloidal systems. The introduction of two different sizes of cylinders has been found to increase the size of band gaps in 2D-PBG crystals.²² The analog here is that introducing extra scattering elements in the unit cell, opens up three-dimensional PBG's. The extra rods or extra cylinders do not lower the crystal symmetry. We also found that the skeletal fcc structure composed of dielectric rods connecting the lattice sites and $f \approx 15\text{--}18\%$ also has a pseudogap (between the 2-3 bands).

We now investigate the “conjugate” fcc structure where the background has high dielectric ($n_b > 1, n_s = 1$). The band structure of close-packed air spheres (dielectric $f=0.26$) generated much initial controversy.^{14–16,20} Full vector-wave band calculations demonstrated that this fcc structure does not have a fundamental gap between the lowest bands. These second and third bands are degenerate at the W point leading to a pseudogap in the photonic DOS (Fig. 3). In addition, the fcc structure has a remarkable full photonic band gap between the 8 and 9 bands, over the entire Brillouin zone (Fig. 3). The magnitude of this gap is largest almost at the close-packed geometry ($f=0.74$), where the low dielectric (air) spheres touch. For all filling ratios, the dielectric background forms a multiply connected network. The minimum refractive index contrast needed to observe this gap is 2.9, somewhat larger than the geometry of spheres and cylinders (Fig. 2). In the close-packed geometry, the gap opens for refractive index contrasts $n_2/n_1 > 2.9$ somewhat larger than that found with dielectric spheres and rods (Fig. 2). Since the higher bands are relatively flat, the band edges are relatively insensitive to the direction of wave propagation.²¹

A process to fabricate the conjugate fcc structure is to use higher dielectric background such as ceramic or semiconductor material enclosing lower dielectric microspheres. A possible high-contrast system consists of filling spaces between polystyrene spheres with semiconductor such as nanocrystalline silicon or germanium and evaporating the spheres to leave a matrix of spherical air cavities in a high dielectric

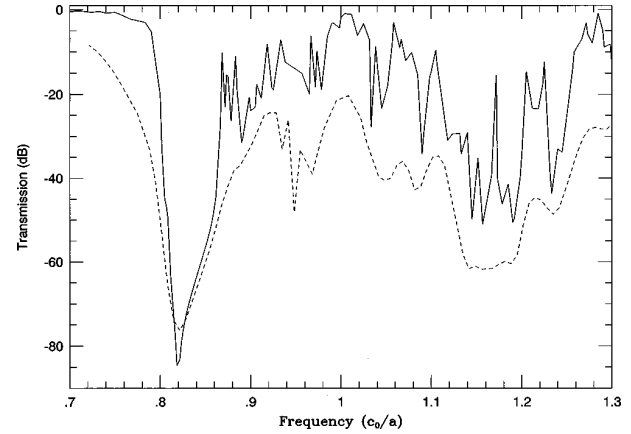


FIG. 4. The transmission along the 100 direction of the fcc crystal of dielectric spheres [DOS in Fig. 1(a)]. Shown are the transmission without absorption (solid line) and a substantial absorption [$\text{Im}(\epsilon)=0.5$] (dashed line). The real part of the dielectric function is kept constant (7.89) in both cases.

background. This would be suitable in the IR region where Si ($n=3.4$) has low absorption, and 0.85μ cavities give the full gap at 1.52μ and the pseudogap at 2.28μ . Using cavities of diameter 310 nm in a background $n=3.1$ (Fig. 3) would give a pseudogap wavelength of 769 nm, and a full gap at 506 nm. These wavelengths simply scale with the size of the cavity. Titania as background ($n=2.81$) can be used for the pseudogap in the optical region.

A dramatic reduction of spontaneous emission would exist within the full band gaps of these fcc structures. Even at the pseudogap of the conjugate structure (Fig. 3), the photon DOS is lower than the free-photon value, and spontaneous emission would also be suppressed. Using higher band gaps increases the frequency by 50% from the lower gap. At the band edges, the fcc DOS is considerably enhanced over the free-photon value due to the higher dielectric material.

We investigate the effect of realistic absorption of the gaps using transfer-matrix calculations. We calculated the transmission along the 100 direction of the fcc crystal of dielectric spheres [$f=0.25$, corresponding to the DOS of Fig. 1(a)], with a substantial absorption [$\text{Im}(\epsilon)=0.5$], and compare it to the case without any absorption (Fig. 4). The low-frequency pseudogap generates a very deep minimum in the transmission (Fig. 4), that is mostly unaffected by absorption. At higher frequencies the transmission is attenuated by 15–20 dB with absorption. The recovery of the transmission after the higher gap is poor, implying that it is difficult to observe higher gaps when absorption becomes significant. We found similar results in transmission calculations through the conjugate fcc structure with absorption. Higher band gaps are more sensitive to absorption since the phase of the electromagnetic wave $\exp(-ink \cdot r)$ oscillates rapidly in the unit cell for higher frequencies or large k , and the wave amplitude is more strongly damped with absorption ($\text{Im} n > 0$). In contrast, the lower band gaps are more robust to absorption and hence easier to measure.

From transfer-matrix calculations we also found that the higher band gap is sensitive to disorder, whereas the pseudogap is far more robust. It is also necessary to maintain the ABC stacking sequence of the close-packed layers to

observe the photonic gaps of the conjugate structure. The alternative hcp structure with *ABAB* stacking does display a higher gap but not the lower pseudogap for the same dielectric contrast used for the fcc structure.

Since we found binary colloidal crystals with full PBG's [the structure in Fig. 1(c)], we investigated the related *AB2* crystal that was experimentally realized in binary mixtures of hard-sphere colloids. In the *AB2* crystal, larger *A* spheres form close-packed layers. The smaller *B* spheres occupy the trigonal prismatic cavities between the *A* layers. The resulting structure consists of alternating hexagonal layers of small and large spheres, with each large sphere surrounded by 12 smaller spheres. We performed calculations for the experimental geometry¹² with radius ratio $R_A/R_B=0.58$, in which the *A* spheres touch.

The photonic DOS for the conjugate *AB2* structure of low dielectric spheres in a high dielectric background ($n_b=3.1, n_s=1$) shows an interesting narrow pseudogap between higher bands [Fig. 5(a)]. The DOS becomes very small over in a narrow high-frequency range is caused by a small number of band crossings occurring at this high frequency. The DOS is below the free-photon value in this frequency range. As found in the fcc and hcp crystals, the "direct" *AB2* structure with high dielectric spheres in a low dielectric background does not exhibit a significant modulation in the photonic DOS [Fig. 5(b)]. The dielectric fraction $f=0.82$ is simply too large.

Generally, photonic band gaps have been found to occur in connected dielectric structures. The *E*-field lines are continuous and the lower "dielectric" band consists of the *E* field concentrated in the dielectric regions. The upper "air" band consists of the *E* field concentrated in the low-dielectric (air) region. The difference between the frequencies of these waves produces the PBG.² This analysis may be extended to gaps at higher frequencies.

In the fcc structure with spheres and cylinders [Fig. 1(b)] or the conjugate fcc structure (Fig. 3), the dielectric region is continuously connected, allowing the distinction between dielectric and air bands. Even in a structure with two dielectric spheres [Fig. 1(c)], a dielectric channel is enhanced by the smaller sphere. Dielectric filling ratios f of 20–30% are optimum. However, for touching dielectric spheres or the *AB2* structure of spheres, the dielectric regions touch at single points, and f is too large to produce gaps. The distinction between dielectric and air bands disappears—all bands are concentrated in the high dielectric region. Connectivity of dielectric structures improves the PBG's as found in other 3D structures.

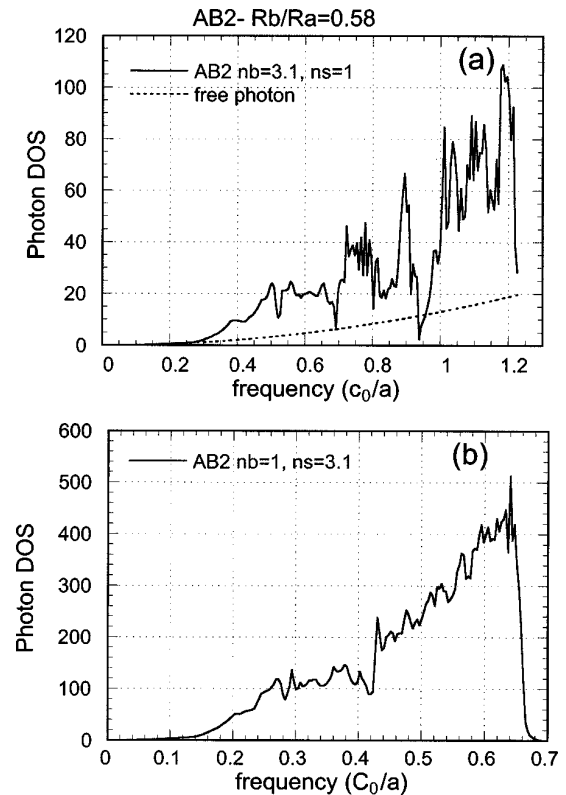


FIG. 5. (a) DOS for the conjugate *AB2* structure with a high dielectric background and air spheres ($n_b=3.1, n_s=1$). The sphere filling ratio is 0.82. For comparison the free photon DOS is shown by the dotted line. (b) DOS for the *AB2* structure with dielectric spheres ($n_s=3.1$) in an air background ($n_b=1$).

In conclusion, we found full three-dimensional photonic band gaps and pseudogaps in fcc structures. Such structures offer interesting possibilities for colloidal crystal growth. Connectivity of the dielectric structure is crucial in opening 3D PBG's. Defect states may be engineered into the gaps by perturbing the lattice periodicity. These systems may have interesting applications in inhibiting spontaneous emission and controlling chemical reactivity.

We thank C. M. Soukoulis and K. Constant for many useful discussions. Ames Laboratory is operated by the U. S. Department of Energy by Iowa State University under Contract No. W-7405-Eng-82. We also acknowledge support by the Department of Commerce through the Center of Advanced Technology Development (CATD) at Iowa State University.

¹For a review see *Photonic Band Gap Materials*, Vol. 315 of NATO Advanced Study Institute, Series E: Applied Sciences, edited by C. M. Soukoulis (Kluwer, Dordrecht, 1996).

²J. D. Joannopoulos, R. D. Meade, and J. N. Winn, *Molding the Flow of Light* (Princeton University Press, Princeton, 1995).

³E. Yablonovitch, *Phys. Rev. Lett.* **58**, 2059 (1987).

⁴J. Martorell and N. M. Lawandy, *Phys. Rev. Lett.* **65**, 1877 (1990).

⁵S. John, *Phys. Rev. Lett.* **58**, 2486 (1987).

⁶V. N. Bogomolov *et al.*, *Appl. Phys. A: Solids Surf.* **63**, 613 (1996).

⁷I. I. Tarhan and G. H. Watson, *Phys. Rev. Lett.* **76**, 315 (1996).

⁸R. Pradhan, J. A. Bloodgood, and G. J. Watson, *Phys. Rev. B* **55**, 9503 (1997).

⁹A. van Blaaderen, R. Ruel, and P. Wiltzius, *Nature (London)* **385**, 321 (1977).

¹⁰P. D. Kaplan, J. L. Rouke, A. G. Yodh, and D. J. Pine, *Phys. Rev. Lett.* **72**, 582 (1994).

- ¹¹A. D. Dinsmore, A. G. Yodh, and D. J. Pine, *Phys. Rev. E* **52**, 4045 (1995).
- ¹²P. Bartlett, R. H. Ottewill, and P. N. Pusey, *Phys. Rev. Lett.* **68**, 3801 (1992), and references therein.
- ¹³S. Fan, P. R. Villeneuve, J. D. Joannopoulos, and E. F. Schubert, *Phys. Rev. Lett.* **78**, 3294 (1997).
- ¹⁴K.-M. Ho, C. T. Chan, and C. M. Soukoulis, *Phys. Rev. Lett.* **65**, 3152 (1990).
- ¹⁵Z. Zhang and S. Satpathy, *Phys. Rev. Lett.* **65**, 2650 (1990).
- ¹⁶K.-M. Leung and Y. F. Liu, *Phys. Rev. Lett.* **65**, 2646 (1990).
- ¹⁷K. Ohtaka and Y. Tanaka, *J. Phys. Soc. Jpn.* **65**, 2265 (1996).
- ¹⁸E. Ozbay, E. Michel, G. Tuttle, M. Sigalas, R. Biswas, and K.-M. Ho, *Appl. Phys. Lett.* **64**, 2059 (1994).
- ¹⁹M. C. Wanke, O. Lehmann, K. Muller, Q. Wen, and M. Stuke, *Science* **275**, 1284 (1997).
- ²⁰H. S. Souzuer, J. W. Haus, and R. Inguva, *Phys. Rev. B* **45**, 13 962 (1992).
- ²¹T. Suzuki and P. K. L. Wu, *J. Opt. Soc. Am. B* **12**, 13 962 (1995).
- ²²C. M. Anderson and K. P. Giapis, *Phys. Rev. Lett.* **77**, 2949 (1996).